

Multichannel Filters Using Chirped Bandgap Structures in Microstrip Technology

Joshua D. Schwartz, *Student Member, IEEE*, Michael M. Guttman, José Azaña, *Member, IEEE*, and David V. Plant, *Fellow, IEEE*

Abstract—We demonstrate two techniques for creating several narrowband transmission channels within the ultra-wide stopband of a chirped electromagnetic bandgap structure in microstrip technology. In contrast to previous demonstrations which inserted defects into single-frequency-tuned bandgap structures using ground-plane etching, we demonstrate the use of local π phase-shifts (defects) and “Moiré”-type superposition in a sinusoidal chirped bandgap structure having a network topology. We demonstrate the design of 4-to-6-channel filters with lower insertion losses (<5 dB) and broader stopbands than previous approaches in microstrip.

Index Terms—Channelizers, microstrip circuits, multichannel resonators, ultra-wideband (UWB) filters.

I. INTRODUCTION

ELECTROMAGNETIC bandgap (EBG) structures have been investigated recently for operation at microwave frequencies, buoyed by potential applications in noise and harmonics suppression in parallel plate technology and antennas, ultra-wideband (UWB) microwave filters, and real-time UWB signal processing [1]–[3]. Microwave EBGs operate by introducing periodic perturbances in metallo-dielectric transmission lines which couple harmonically resonant input frequencies to their counter-propagating modes, creating a reflecting bandgap region.

It is well-known that by breaking the periodicity of this bandgap structure (e.g. by inserting a local defect), a resonant transmission peak occurs within the bandgap. This transmission can be understood from the point of view of coupled-mode theory: electromagnetic waves experiencing Bragg-like reflection from a periodic structure encounter a $\pi/2$ shift each time they reflect. If a defect were introduced, this amounts to a phase-shift in the periodicity, and for a certain frequency within the bandgap this will correspond to a full π phase-shift. This shift will add to the existing π phase-shift experienced by any twice-reflected waves at that particular frequency, constructively supporting a forward propagating wave in a narrow

bandwidth. By using different shapes and sizes of defects, multiple resonant channels can be created within the bandgap region [4].

Other channelizers that have been demonstrated using defect-insertion include multipath topologies [5], and drop-filter structures which isolate different channels at dedicated ports [6]. Unfortunately, the channels demonstrated in [4] and [5] experienced insertion losses in excess of 10 dB, with bandwidths below 3 GHz, and the approach of [6] consumes significant board area for multichannel operation since it requires a dedicated EBG for each dropped frequency. Here, instead of inserting different defects into a single-frequency EBG pattern, we introduce the same kind of defect (a local π phase-shift) into a structure whose local period is continually changing (i.e., chirped). This approach dramatically improves channel transmission and stopband bandwidth while reducing the number of etching steps required to one, since the EBG is written in the conductor strip instead of the ground plane.

It has also been demonstrated that EBGs of different periodicities may be superimposed in summation instead of being concatenated sequentially, resulting in multiple-tuned stopbands [7]. Although that work employed multiple single-frequency EBG structures, we will demonstrate that by superimposing chirped EBGs, a multichannel filter emerges within a single broad stopband, emulating a structure known in photonics as a “chirped Moiré” fiber grating. These Moiré structures exhibit slightly broader bandwidths and less rippled response than locally defected EBGs.

In Section II of this work, we introduce the design of multichannel filters using defected chirped EBG structures in microstrip. Section III details the alternative “chirped Moiré” approach. Finally, Section IV contains simulation and measurement results for designs using both configurations.

II. DEFECTED CHIRPED EBG STRUCTURES

It was demonstrated by Laso *et al.* [8] that the total effective bandwidth of an EBG structure may be increased by introducing chirp. A continuous strip-width modulation can be etched into the strip conductor of a microstrip to create a smoothly-varying impedance profile of the form

$$Z_0(z) = 50 \cdot \exp[A \cdot Y(z)] \quad (1)$$

where “A” controls the depth of the modulation and $Y(z)$ is a chirped sinusoid

$$Y(z) = \sin\left(\left(\frac{2\pi}{a_0} + C \cdot z\right) \cdot z - C \frac{L^2}{4}\right). \quad (2)$$

Manuscript received February 1, 2007. This work was supported in part by the Natural Sciences and Engineering Research Council of Canada (NSERC).

J. D. Schwartz and D. V. Plant are with the Photonics Systems Group, Department of Electrical and Computer Engineering, McGill University, Montreal, QC H3A 2A7, Canada (e-mail: joshua.schwartz@mcgill.ca).

M. M. Guttman is with the Microelectronics and Computer Systems laboratory, Department of Electrical and Computer Engineering, McGill University, Montreal, QC H3A 2A7, Canada.

J. Azaña is with the Institut National de la Recherche Scientifique-Energie, Matériaux et Télécommunications (INRS-EMT), Montréal, QC H5A 1K6, Canada (e-mail: azana@emt.inrs.ca).

Digital Object Identifier 10.1109/LMWC.2007.901765

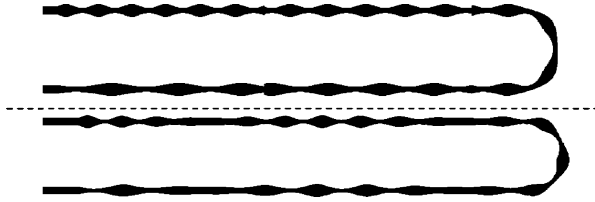


Fig. 1. Four-channel phase-shifted (top) and Moiré (bottom) microstrips, 18.9 cm long, with channels at 5.35 GHz, 6.45 GHz, 7.5 GHz, and 8.6 GHz. The meandered shape of the structures was to fit a 10 cm etching process.

The form in (1) of a raised sinusoid is chosen for its rejection of higher-order harmonics. The device extends from $z = -L/2$ to $+L/2$ with a central period “ a_o ” (at $z = 0$) and a chirp parameter “ C ” (m^{-2}) describing the rate of change of the locally reflected frequency $f(z)$

$$f(z) = \frac{c}{4\pi\sqrt{\epsilon_{eff}}} \left(\frac{2\pi}{a_o} + 2 \cdot C \cdot z \right). \quad (3)$$

At any location along the structure, a resonant channel at the local frequency $f(z)$ can be obtained by adding a π phase-shift to $Y(z)$. Each inserted π -shift corresponds to one local frequency. Other phase-shifts besides π may be used (this is effectively the method used in [4]), the effect of which is to translate the resonance away from the local frequency. Many channels can be created within a single chirped structure; the four-channel device demonstrated here is illustrated in Fig. 1 (top). The principle drawback of EBG structures is, in general, their length; chirped EBGs can run into the tens of centimeters. Shorter structures are possible with thin, high-permittivity substrates, and the authors suspect that stripline-geometry structures will demonstrate improved performance.

III. CHIRPED MOIRÉ STRUCTURES

In the context of optical fiber-Bragg gratings, fabrication difficulties surrounding the insertion of local phase-shifts into gratings spurred the development of an alternative approach for generating local π phase-shifts: the chirped superposition or “Moiré” structure [9]. By superimposing two sinusoidal patterns with the same chirp but differing central frequencies, the resulting sum is also chirped and contains evenly-spaced crossover points or “beats,” where the phase-shift naturally changes by π . This can be achieved in microstrip using (1) by choosing the following form for $Y(z)$:

$$Y(z) = \sin \left(\left(\frac{2\pi}{a_{o1}} + C \cdot z \right) \cdot z - C \frac{L^2}{4} \right) + \sin \left(\left(\frac{2\pi}{a_{o2}} + C \cdot z \right) \cdot z - C \frac{L^2}{4} \right). \quad (4)$$

Periods a_{o1} and a_{o2} correspond to the central ($z = 0$) frequencies f_{o1} and f_{o2} of two independent stopbands. Their average determines the center frequency of the summation stop-band, which is wider than that of a single chirped pattern. An illustration of a Moiré structure with four “beats” is shown in Fig. 1 (bottom). The number of resonant peaks, the distance between adjacent peaks, and the width of the rejection bandgap can be

designed based on the device length. The frequency-spacing between resonant transmission peaks is determined by the chirp and the physical length between beats, Δz , which is a function of the choice of central periods

$$\Delta\omega = \frac{c}{\sqrt{\epsilon_{eff}}} \cdot C \cdot \Delta z = \frac{c}{\sqrt{\epsilon_{eff}}} \cdot C \cdot \frac{a_{o1} \cdot a_{o2}}{|a_{o1} - a_{o2}|}. \quad (5)$$

The number of channels (beats) “ n ” is then dependent on the length of the structure

$$n = 2 \cdot \text{int} \left(\frac{L}{2} \cdot \frac{|a_{o1} - a_{o2}|}{a_{o1} \cdot a_{o2}} \right). \quad (6)$$

Unlike the local-defect insertion technique, these channels are of necessity evenly-spaced within the bandgap.

IV. SIMULATION AND EXPERIMENTAL RESULTS

Our designs employed a medium-quality alumina substrate with permittivity $\epsilon_r = 9.41$, $\tan \delta = 0.0007$, and thickness 1.27 mm, metallized with a gold alloy. The designs were simulated using Agilent’s Momentum software (a 2.5D Method of Moments solver) including substrate and conductor losses. Test structures were fabricated and their S -parameters measured with a vector network analyzer.

The phase-shifted implementation featured four equally-spaced π -shifts along a microstrip of length $L = 18.9$ cm with a central period of $a_o = L/23 = 0.82$ mm, $A = 0.24$ and chirp $C = -1600$ m^{-2} for an effective bandgap from 4.5 to 10.5 GHz. Simulation and measurement S -parameter data are presented in Fig. 2 and show very close agreement. The interchannel spacing is approximately 1.1 GHz and the 3-dB bandwidth of these channels is 150–200 MHz. Channel insertion losses are approximately 2–3 dB, a significant improvement over the values in [4] and [5] which exceeded 10 dB. The depth of channel isolation, defined here as the difference between the transmission peak and the neighboring valley, varies from 8 to 22 dB and generally improves towards the higher frequencies—this is a characteristic of linearly chirped EBG structures, which have fewer periods at low frequencies and therefore exhibit weaker reflectivity. This situation can be improved by using an asymmetrical tapering window [8]. To illustrate the correspondence between each phase-shift and a corresponding channel, Fig. 3 illustrates the same design with the third phase-shift removed, eliminating one channel.

For comparison, we also designed a chirped-Moiré four-channel structure of the same length, having central frequencies $a_{o1} = L/21$ and $a_{o2} = L/26$. As shown in Fig. 4, this achieves a slightly broader but shallower rejection band, resulting in slightly reduced depth of isolation compared to the phase-shift method. We can control the number of channels with the spacing of the central period, demonstrated by Fig. 5, in which we push apart the central periods apart to $a_{o1} = L/20$ and $a_{o2} = L/27$ while retaining the same overall bandgap frequency. The result features six beats in the Moiré pattern and thus six channels are evident, although the lowest-frequency channel suffers from poor isolation because of the weak number of periods there. While the local-phase-shift approach offers flexibility of channel location, the Moiré method favors broader,

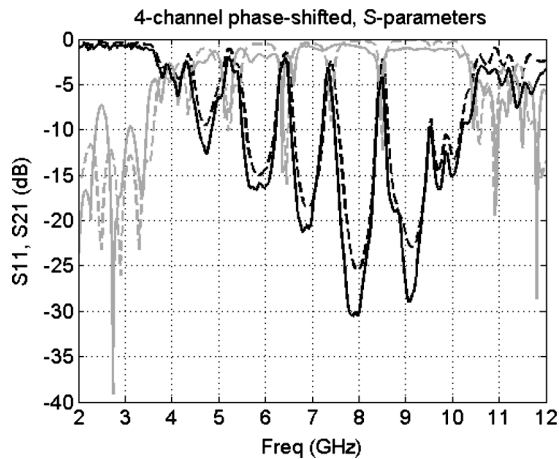


Fig. 2. S11 (grey) and S21 (black) data from simulation (dash) and measurement (solid) for a chirped EBG structure with four evenly distributed local π phase-shifts ($A = 0.24$, $C = -1600 \text{ m}^{-2}$, $L = 18.9 \text{ cm}$, $f_0 = 7 \text{ GHz}$).

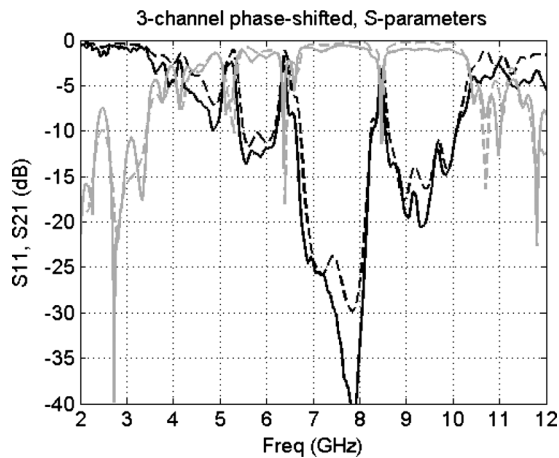


Fig. 3. S11 (grey) and S21 (black) data from simulation (dash) and measurement (solid) for the chirped EBG structure described in Fig. 3 with the third phase-shift removed.

shallower stopbands and exhibits a less rippled response due to smoother impedance profiles.

ACKNOWLEDGMENT

The authors wish to thank Dr. T. Le-Ngoc and R. Morawski for their assistance in providing access to vector network analysis equipment.

REFERENCES

- [1] R. Abhari and G. Eleftheriades, "Metallo-dielectric electromagnetic bandgap structures for suppression and isolation of the parallel-plate noise in high-speed circuits," *IEEE Trans. Microw. Theory Tech.*, vol. 51, no. 6, pp. 1629–1639, Jun. 2003.
- [2] J. Schwartz, J. Azaña, and D. V. Plant, "Real-time microwave signal processing using microstrip technology," in *IEEE MTT-S Int. Dig.*, Jun. 2006, pp. 1991–1994.
- [3] J. Schwartz, J. Azaña, and D. V. Plant, "A fully-electronic system for the time-magnification of ultra wideband signals," *IEEE Trans. Microw. Theory Tech.*, vol. 55, no. 2, pp. 327–334, Feb. 2007.

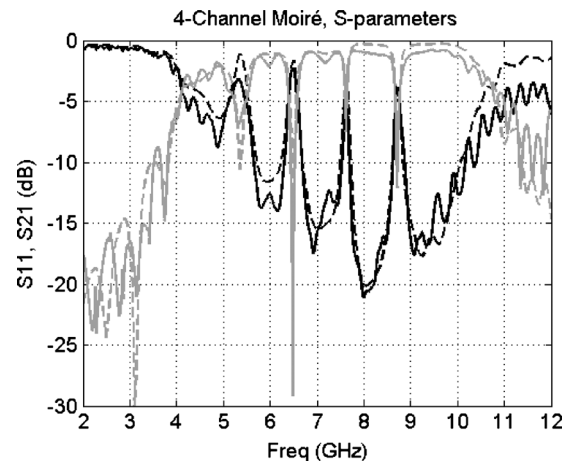


Fig. 4. S11 (grey) and S21 (black) data from simulation (dash) and measurement (solid) for a four-channel chirped Moiré EBG structure ($A = 0.14$, $C = -1718 \text{ m}^{-2}$, $L = 18.9 \text{ cm}$, $f_1 = 6.43 \text{ GHz}$, $f_2 = 7.96 \text{ GHz}$).

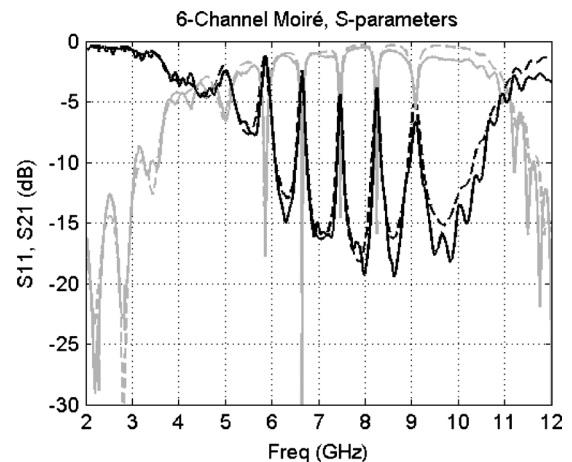


Fig. 5. S11 (grey) and S21 (black) data from simulation (dash) and measurement (solid) for a six-channel chirped Moiré EBG structure ($A = 0.14$, $C = -1718 \text{ m}^{-2}$, $L = 18.9 \text{ cm}$, $f_1 = 6.12 \text{ GHz}$, $f_2 = 8.27 \text{ GHz}$).

- [4] A. Griol, D. Mira, A. Martinez, and J. Marti, "Multiple-frequency photonic bandgap microstrip structures based on defects insertion," *Microw. Opt. Technol. Lett.*, vol. 36, no. 6, pp. 479–481, Mar. 2003.
- [5] Y. Li, H. Jiang, L. He, H. Li, Y. Zhang, and H. Chen, "Multichanneled filter based on a branchy defect in microstrip photonic crystal," *Appl. Phys. Lett.*, vol. 88, pp. 1–3, Feb. 2006.
- [6] C.-S. Kee, I. Park, and H. Lim, "Photonic crystal multichannel drop filters based on microstrip lines," *J. Phys. D (Appl. Phys.)*, vol. 39, no. 14, pp. 2932–2934, Jul. 2006.
- [7] M. A. G. Laso, T. Lopetegui, M. J. Erro, D. Benito, M. J. Garde, and M. Sorolla, "Multiple-frequency tuned photonic bandgap microstrip structures," *IEEE Microw. Guided Wave Lett.*, vol. 10, no. 6, pp. 220–222, Jun. 2000.
- [8] M. A. G. Laso, T. Lopetegui, M. J. Erro, D. Benito, M. J. Garde, M. A. Muriel, M. Sorolla, and M. Guglielmi, "Chirped delay lines in microstrip technology," *IEEE Microw. Wireless Compon. Lett.*, vol. 11, no. 12, pp. 486–488, Dec. 2001.
- [9] L. A. Everall, K. Sugden, J. A. R. Williams, I. Bennion, X. Liu, J. S. Aitchison, and R. M. De La Rue, "Fabrication of in-line Moiré filters using a 5-cm nondedicated chirped phase mask," *Bragg Gratings, Photosens., Poling Glass Fibers Waveguides: Appl. Fund.*, vol. 17, pp. 228–230, 1997.